Participation of Ras and Extracellular Regulated Kinase in the Hyperplastic Response of Middle-Ear Mucosa during Bacterial Otitis Media

Sean D. Palacios,[1,a] Kwang Pak,[1,a] Ayse G. Kayali,[2] Alexander Z. Rivkin,[1] Christoph Aletsee,[3] Åsa Melhus,[4] Nicholas J. G. Webster,[2] and Allen F. Ryan[1]

Departments of [1]Head and Neck Surgery and [2]Medicine, University of California, San Diego, School of Medicine, La Jolla; [3]University of Würzburg, Department of Otolaryngology, Würzburg, Germany; [4]Department of Microbiology, University of Lund, Lund, Sweden

Hyperplasia of middle-ear mucosa (MEM) during otitis media (OM) is thought to be partially mediated by the actions of growth factors and their receptors. The intracellular pathway leading from the small G-protein Ras to the extracellular regulated kinases (Erks) often links growth factor stimulation to cellular proliferation. This study assessed whether this pathway is involved in MEM hyperplasia during bacterial OM via the activation of Erk1/Erk2 in MEM of an in vivo rat bacterial OM model. Activation was maximal at 1 and 6 h and at 1 week after introduction of bacteria into the middle ear. Additionally, an in vitro model of rat MEM in bacterial OM was treated with farnesyl transferase inhibitor 277 or the Mek inhibitor U0126. MEM explants treated with either inhibitor demonstrated significant suppression of bacterially induced growth. These data support a role for Ras and Erk signaling in MEM hyperplasia during bacterial OM.

Otitis media (OM) leads to conductive hearing loss that develops secondary to damage caused by transformation of the inflamed middle-ear mucosa (MEM). Normally, the MEM consists of a simple squamous epithelium overlying a thin lamina propria that adheres to the underlying periostium [1]. This monolayer of epithelial cells ranges from 15–20 μm thick but has the unique capacity to grow and proliferate into a highly structured, pseudostratified, columnar epithelial complex that can be >1000 μm thick [2–5]. The hyperproliferative response is activated rapidly after any number of OM-related stimuli, including tubal obstruction [6], bacteria [7, 8], endotoxin [9, 10], immunologic challenge [5, 11], and cytokines [12]. Middle-ear effusion, atelectasis, adhesive otitis, tympanic membrane perforation, tympanosclerosis, scarring of the MEM, and cholesteatoma are the major forms of morbidity associated with OM [13–18]. These pathologic conditions can lead to permanent damage of the middle-ear cavity, resulting in hearing loss or impairment [5]. Understanding the intracellular pathophysiological mechanisms responsible for this hyperplastic response may enable us to treat OM before such irreversible damage takes place.

In most complex organisms, growth of dividing cells is controlled, in part, by growth factors. Earlier investigations have suggested that growth factors, specifically the epidermal growth factor (EGF) and fibroblast growth factor (FGF) families, are involved in the proliferation of the MEM during OM [2, 3, 19–22]. The EGF and FGF receptors are protein tyrosine kinases that contain an extracellular ligand-binding domain, a transmembrane domain, and a cytoplasmic portion. Ligand binding to the extracellular domain leads to receptor dimerization and phosphorylation that ultimately opens docking sites for adaptor proteins to the cytoplasmic portion of the receptor [23]. These adaptor proteins, with the aid of nucleotide exchange factors (GEFs), can convert guanine diphosphate (GDP)–Ras, a guanine-nucleotide binding protein, to active guanine triphosphate (GTP)–Ras, which controls intracellular signaling pathways that regulate diverse cellular functions, including growth and proliferation [24]. Overexpression of this protein even mimics the effects of continued activation of growth factor receptors such as FGFR, EGFR, and platelet-derived growth factor receptor [25, 26].

GTP-Ras is believed to partially mediate cellular proliferation by activation of the downstream effector protein Raf (MAP kinase kinase kinase). Raf is the first of a cascade of downstream kinases that also includes Mek (MAP kinase kinase) and extracellular regulated kinase 1 (Erk1)/Erk2 (MAP kinase), respectively [27]. Once Erks are activated, they translocate to the nucleus and modulate gene expression [28]. Although Ras is a cytoplasmatic protein, interaction with cell-membrane lipids is required for its cellular activity. For Ras to be activated, a posttranslational farnesylation to the C-terminus, catalyzed by farnesyl transferase, must take place [29]. This

Received 17 October 2001; revised 26 July 2002; electronically published 22 November 2002.

Presented in part: Winter meeting of the Association for Research in Otolaryngology, St. Petersburg, Florida, 4–8 February 2001 (abstract 738).

All experiments were performed according to National Institutes of Health (NIH) guidelines on the care and use of laboratory animals and were approved by the institutional committee for animal experimentation.

Financial support: NIH/NIDCD (DC00129); Research Service of the US Department of Veteran Affairs.

[a] The first 2 authors contributed equally to the manuscript.

Reprints or correspondence: Dr. Allen F. Ryan, University of California, San Diego, School of Medicine, Fir Bldg., Rm. 106, 9500 Gilman Dr. #0666, La Jolla, CA 92037 (afryan@ucsd.edu).

The Journal of Infectious Diseases 2002; 186:1761–9

0022-1899/2002/18612-0010$15.00

farnesylation mobilizes GDP-Ras to the plasma membrane [30]. Receptor tyrosine kinase activation can then activate Ras to the GTP form by means of GEFs. Active farnesylated GTP-Ras is then free to bind to and translocate Raf to the plasma membrane and start the MAP kinase cascade leading to cellular proliferation. If cytoplasmatic Ras is not anchored to the plasma membrane, it can still be activated to its GTP form. This free cytoplasmatic GTP-Ras can still bind the Raf protein, forming inactive Ras/Raf complexes. These complexes disrupt the activation of all Ras-specific downstream effector pathways, including the Ras/Erk signaling cascade [31].

The Ras/Erk intracellular pathway, in conjunction with growth factor tyrosine kinase receptors, has been shown to influence epithelial cellular proliferation in other tissue systems [26, 32, 33]. Therefore, it is likely that this same pathway may be linked to the effectiveness of the growth factors responsible for the hyperplastic response of the MEM during bacterial OM. For this reason, we developed an in vitro model of bacterially induced hyperplasia in rat MEM. Farnesyl transferase inhibitor (FTI)–277 and the Mek/Erk inhibitor U0126 were used to explore the role of Ras in mediating cellular growth and proliferation in this hyperplastic and in a nonhyperplastic in vitro mucosal model. We also evaluated the activation of Erk1 and Erk2 at 7 postinfection time points in an established rat in vivo model of bacterial OM [8, 34, 35]. The combined data from our study provide information about the role played by Ras and Erks in the hyperplastic response of the MEM during bacterial OM.

Materials and Methods

Hyperplastic middle ear mucosa in vitro model. Sixteen male Sprague-Dawley rats weighing 300–350 g were anesthetized with a mixture of ketamine and xylazine at 100 mg/mL and acepromazine at 10 mg/mL, injected intramuscularly at a dose of 0.4 mL/100 g. On sedation, the animals were placed in the supine position and their bodies stabilized with masking tape. A 3-cm, vertical, midline incision was made between the animal's mandible and clavicles, and middle-ear bullae exposure was obtained bilaterally with the aid of a dissecting microscope. A 25-gauge syringe needle was used to fenestrate the center of the middle-ear bullae bilaterally. A solution containing 10^5 *Haemophilus influenzae* strain 3655 (nontypeable, biotype II) cells/mL was then injected bilaterally into the middle-ear bullae until the solution overflowed the fenestrations. Excess fluid was absorbed with a cotton swab. The original fascia covering the middle-ear bulla was then used to recover the hole in the bone, and the incisions were stapled closed. Each animal was examined to guarantee that their tympanic membranes had not been ruptured. The rats were divided into 4 groups of 4 animals each. Each group was anesthetized and killed by decapitation at 1 of 4 time points. The time points included 6, 24, 48, and 120 h after inoculation. After each group of animals was killed, the middle-ear bullae were surgically extracted. The bullae were immediately opened and placed in a Petri dish containing warm PBS. The MEMs were surgically removed intact from the anteriolateral part of the bullae. Each MEM sample was immediately placed in a separate 60-mm Falcon petri dish coated with a thin layer of Sylgard 184 silicone elastomer (Dow Corning). Culture medium, consisting of a mixture of Dulbecco's modified Eagle's medium and Ham's F12 medium (3:1) supplemented with fetal calf serum (5%), hydrocortisone (0.4 μg/mL), isoproterenol (10^{-6} *M*), penicillin (100 U/mL), and streptomycin (100 μg/mL), was then added [22]. The MEMs were divided into ~1-mm^2 tissue explants, using a Fine Science Tools diamond knife. The explants from each bulla were then individually transplanted, epithelium uppermost, into single wells of a 24-well Falcon cell culture plate containing 170 μL of culture medium. They were placed in an incubator at 37°C with 5% CO_2 for 24 h and allowed to adhere to the culture plate surface. After 24 h, 500 μL of culture medium was added to each well, and the plates were replaced in the incubator for 72 h. On day 4, each well was individually examined with a microscope under 40× magnification. The culture medium was changed in all wells with healthy, attached explants, and the plates were replaced in the incubator. On day 8, the medium was changed once again. The middle-ear bullae from an additional 4 uninfected rats were dissected and treated in the manner described above, to serve as a negative control.

The tissue explants were immunohistochemically stained with an anti–5-bromo-2-deoxyuridine (BrdU) primary antibody (Sigma-Aldrich) followed by a biotinylated secondary antibody (Santa Cruz Biotechnologies). After the appropriate biotin and avidin blocks, the cultures were treated with a fluorescein isothiocyanate (FITC)–labeled strepavidin (DAKO). Each well was then photographed with a green flourescent protien (GFP) filter.

Only explants that maintained a healthy appearance and remained firmly attached to the well surface throughout the entire duration of the study were used. For each time point, 8–18 explants were photographed each day, for 10 days, with the aid of a Leica dissecting microscope at 2.64× magnification under standard exposure conditions. Because the outgrowth from each explant was approximately circular, the diameter of the outgrowths was measured and their surface areas were calculated to document tissue explant growth. The data were entered into Statview 5.0, and an analysis of variance (ANOVA) was run. $P < .05$ was considered to be statistically significant.

Treatment with Ras inhibitor FTI-277 and Mek/Erk inhibitor U0126. The bullae of 6 male Sprague-Dawley rats weighing 300–350 g were injected with *H. influenzae* strain 3655 (nontypeable, biotype II) at 10^5 cells/mL in the manner described above. After 48 h, the rats were killed, and the MEM were dissected, cut into 1-mm^2 explants, and cultured as described above. On day 1, all wells with healthy, attached explants were randomly divided into 4 groups. The Ras inhibitor FTI-277 (Calbiochem) was reconstituted in DMSO (Sigma-Aldrich) and added, at 1, 10, or 20 μM, respectively, in 300 μL of culture medium. The last group served as a negative control; a supplement of 1 μL/mL of DMSO alone was added to the medium. The same concentration of DMSO was used for all concentrations of FTI-277. Every day, all of the medium from each well was removed, and 300 μL of fresh culture medium was added with the appropriate concentration of FTI-277 and/or DMSO. One-half the explants from each group were also treated with BrdU every day for the entire duration of the experiment. The other half from each group was daily treated with BrdU, starting on day 6 of the experiment. All explants were maintained in culture for 10 days. Using the same procedures, explants were

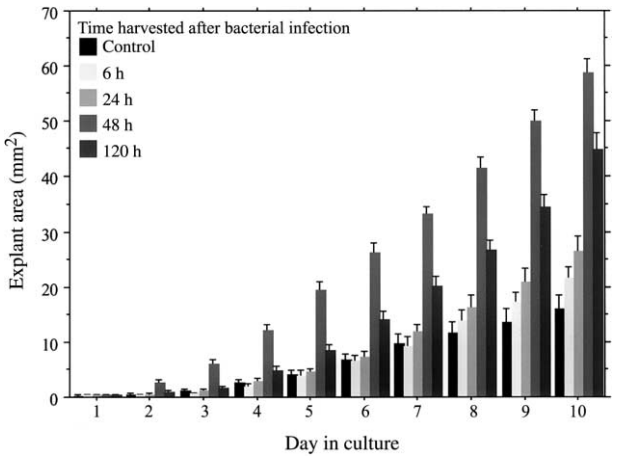

Figure 1. Surface area measurements of in vitro middle-ear mucosa explants harvested at the indicated postinoculation times and cultured for 10 days. Maximal growth was observed in mucosal explants harvested 48 h after bacterial inoculation of the middle ear. Bars, means; vertical lines, 1 SE.

cultured with the Mek inhibitor U0126 (Calbiochem) at 10, 100, and 1000 n*M*.

For each individual inhibitor concentration, 6–10 explants were photographed daily with an RT color digital camera and their surface areas were calculated using SPOT computer software calibrated to the appropriate magnification. The data were entered into Statview 5.0, and an ANOVA was run. The tissue explants were also immunohistochemically stained with an anti-BrdU primary antibody. The cultures were then treated with a biotinylated secondary antibody. After the appropriate biotin and avidin blocks, the cultures were treated with an FITC-labeled strepavidin. Each well was then photographed again under varying magnifications with a GFP-2 fluorescent filter.

Inhibition of nonhyperplastic mucosae with FTI-277 and U0126. The MEMs of 12 male Sprague-Dawley rats that had not been infected with *H. influenzae* were dissected, divided, and cultured in the manner described above. The explants were divided into 7 groups. One group each was cultured with 10 and 20 μM FTI-277 and 10, 100, and 1000 n*M* U0126. Two groups were cultured with 1 μL/mL DMSO, the same concentration of DMSO used for all concentrations of the inhibitors, as control specimens. The cultured tissue was cared for and photographed as described above for 10 days. For each individual inhibitor, 10–14 explants were evaluated. Because the effects of the inhibitors did not appear to differ across the 10-day period studied in our experimental cultures, growth was evaluated on only a subset of culture intervals: explant outgrowth surface areas were measured from the photographs on days 1, 3, 7, and 10. An ANOVA was run.

Assessment of ERK phosphorylation. The bullae of 21 male Sprague-Dawley rats weighing 300–350 g were injected with *H. influenzae* strain 3655 (nontypeable, biotype II) at 10^5 cells/mL in the manner described above. The MEMs were dissected bilaterally from 3 rats at 1 of 7 time points. The time points were 1, 6, 24, 48, and 72 h and 6 and 7 days after infection. These times were chosen on the basis of the results of Magnuson et al. [8], who found that mucosal hyperplasia was maximal at 4 days and had partially recovered by 8 days after inoculation of the middle-ear with *H. influenzae* . The MEMs from 3 control rats were also dissected bilaterally. All the MEMs were immediately frozen at −70°C.

The frozen tissue was homogenized in 100 μL of radioimmunoprecipitation buffer that contained 20 m*M* Tris (pH 7.5), 1 m*M* EDTA, 140 m*M* NaCl, 1% Nonidet P-40, 1 m*M* sodium orthovanadate, 1 m*M* phenylmethylsulfonyl fluoride, 50 m*M* sodium fluoride, and 10 μg/mL aprotinin, using a Potter-Elvhejlm homogenizer. The homogenates were centrifuged at 14,000 *g* at 4°C, and the pellets were discarded. Twenty-five micrograms of protein from each sample were mixed with 2× SDS sample buffer. The samples were boiled, and the proteins were resolved on 10% SDS–polyacrylamide gel electrophoresis. After being transferred to polyvinylidine fluoride paper, the proteins were immunoblotted with rabbit polyclonal antibodies to active Erk (Promega). The anti–active Erk antibody was generated using a dual phosphorylated peptide derived from the catalytic region of MAP kinase, corresponding to Thr183 and Tyr185 of the mammalian Erk2 enzyme and used at a dilution of 1:20,000. After incubation with secondary horseradish peroxidase–conjugated anti-rabbit antibodies, the proteins were visualized by enhanced chemiluminescence (Pierce). The blot was stripped and reprobed with anti–total Erk antibody (Promega) and then restripped and probed with an anti-p38 antibody (Promega).

Measurement of lactate dehyrdogenase (LDH) release after treatment with maximum doses of FTI-277 and U0126. MEM explants of 2 male Sprague-Dawley rats were cultured 48 h after injections with *H. influenzae.* Three groups of 10 explants each were treated with DMSO, 10 μM FTI-277, or 1000 n*M* U0126 for 10 days, with daily media change. The medium was collected from each explant on days 1, 3, 7, and 10. Percentage cytotoxicity was then measured using the CytoTox 96 Non-Radioactive Cytotoxicity Assay kit (Promega), and the absorbance was recorded at 490 nm.

Expression of Ras isoforms in hyperplastic MEM. The bullae of 2 male Sprague-Dawley rats weighing 300–350 g were injected with *H. influenzae* strain 3655 (nontypeable, biotype II) at 10^5 cells/mL in the manner described above. After 48 h, the middle-ear bullae were surgically extracted bilaterally from each animal. The bullae were immediately opened and placed in a petri dish containing warm PBS. The MEMs were surgically removed intact from the anteriolateral bullae. Each MEM sample was immediately placed in a 1.5-mL eppendorf tube and stored at −70°C.

The MEMs were homogenized, and reverse-transcriptase polymerase chain reaction (RT-PCR) was performed using Dynabeads Oligo $(dT)_{25}$ (Dynal). The resulting cDNA was used for PCRs with 3 different primer sets (Oligos) corresponding to the different isoforms of rat Ras: H-Ras, N-Ras, and K-Ras. The size of the PCR products was then analyzed by means of agarose gel electrophoresis.

Results

Appearance of mucosa in situ in the middle ear. Before dissection into explants, the extracted MEMs were examined under a dissecting microscope. On extraction from the bullae, the MEMs were progressively thicker as the bacterial exposure in vivo increased. Six hours after infection, the MEMs were comparable in thickness and behavior during dissection to the neg-

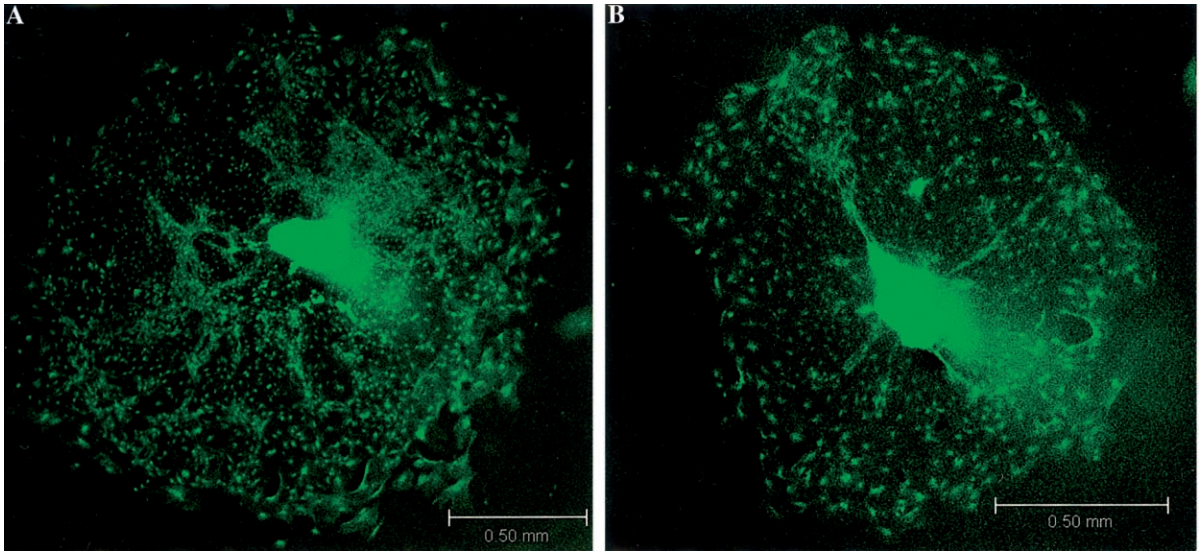

Figure 2. Representative middle-ear mucosal explants and outgrowth after treatment with 5-bromo-2-deoxyuridine (BrdU) starting on days 1 *(A)* and 6 *(B)* of 10 days of culture, stained with fluorescine isothiocyanate–labeled anti-BrdU. Virtually all nuclei are labeled.

ative control specimens. At 24 h, the MEMs were thicker, and they tolerated manipulation better than the negative control specimens. This was also the case at 48 h. However, beyond 48 h, there appeared to be an increase in the fragility of the tissue. At 72 h, mucosal thickening had not changed but the ability of the tissue to tolerate manipulation was low, and intact explants could not be obtained. The thickness at 120 h was less than that at 48 h. The tissue was fragile, but intact explants could be obtained with some difficulty.

In vitro MEM hyperplasia. The growth and appearance of cultured mucosal explants from uninfected middle ears were similar to that described elsewhere [19]. The explants contained both epithelial and underlying stromal cells. However, the culture conditions favored the growth of epithelial cells. In our previous study, when explants were stained with antibodies specific for epithelial cytokeratins, almost all cells were labeled [19]. Bacterial infection of the middle ear substantially altered the growth of mucosal explants. Figure 1 illustrates the average surface area of the cultured MEM samples for the 4 *H. influenzae,* in vivo, exposure time points, and the negative control. When cultured in vitro, tissue explants exposed to bacteria in vivo for 48 h had the greatest hyperplastic response in comparison to the negative control. Tissue explants cultured after 120 h also displayed a significant increase in surface area compared with the negative control, but the increase was not as extensive as that at 48 h.

BrdU. The explants treated with BrdU for the duration of the study demonstrated BrdU-positive staining throughout the entire outgrowth. The majority of tissue explants treated with BrdU starting on day 6 also demonstrated BrdU-positive nuclei uniformly throughout the outgrowth, similar to the explants treated with BrdU starting from day 1. The results are shown in figure 2.

Ras inhibition with FTI-277 and Mek inhibition with U0126 in hyperplastic MEMs. Figure 3 illustrates the effects of the Ras farnesylation inhibitor FTI-277 and the Erk inhibitor U0126 on the surface area of the cultured hyperplastic MEM explants. All examined explants maintained a healthy appearance and remained firmly attached to the plate surface throughout the entire duration of the study. As illustrated in figure 3*A,* FTI-277 at 1 μM did not have a significant inhibitory effect ($P < .2564$) on tissue outgrowth. By day 10 of the study, FTI-277 at 10 μM had a significant inhibitory effect ($P < .0001$), decreasing outgrowth surface area by 75%, compared with the negative control specimens. FTI-277 at 20 μM had a similar effect ($P < .0001$), decreasing outgrowth surface area by 74%, compared with the negative control specimens. However, when compared with each other, there was no significant difference between explant outgrowths treated with 10 and 20 μM FTI-277. As shown in figure 3*B,* no inhibition by U0126 was observed at 10 nM and 100 nM ($P < .3201$ and $P < .9864$, respectively). However, 1000 nM U0126 decreased outgrowth surface area by 45% ($P < .0001$).

Ras inhibition with FTI-277 and Mek inhibition with U0126 in nonhyperplastic MEMs. Figure 4 illustrates the effects of FTI-277 and U0126 on the surface area of the cultured nonhyperplastic MEM explants. By day 10, FTI-277 at 10 μM had a significant inhibitory effect ($P < .0002$), decreasing tissue outgrowth by 29%, compared with the negative control specimens. FTI-277 at 20 μM also had an inhibitory effect ($P < .0001$), decreasing outgrowth surface area by 38%, compared with the negative control specimens. Compared with each other, there was no significant difference between explant outgrowths

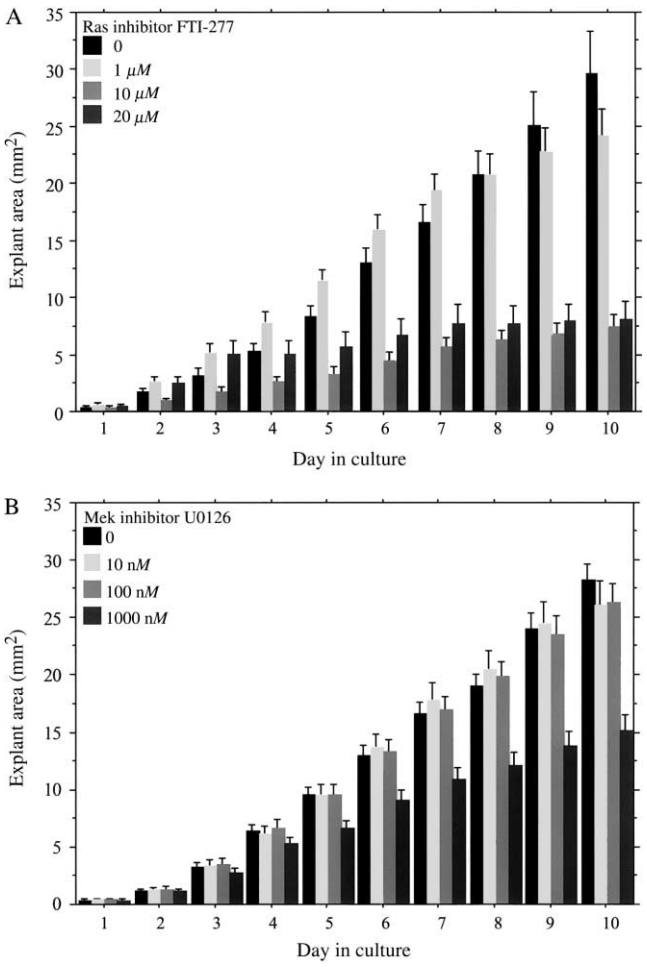

Figure 3. Surface area of hyperplastic middle-ear mucosa explants (all harvested 48 h after bacterial inoculation of the middle ear) cultured with different concentrations of signaling inhibitors. *A,* With farnesyl transferase inhibitor (FTI) 277, significant inhibition of growth was observed at 10 μM ($P < .0001$) and 20 μM ($P < .0001$). *B,* With the Mek inhibitor U0126, significant inhibition of growth was observed at 1000 nM ($P < .0001$). Bars, means; vertical lines, 1 SE.

treated with 10 and 20 μM FTI-277 (figure 4*A*). All concentrations of U0126 resulted in significant inhibition of explant outgrowth (34%, 50%, and 59%; $P < .0001$; figure 4*B*).

Measurement of LDH release after treatment with FTI-277 and U0126. All the explants treated with maximum doses of the inhibitors showed no significant LDH release in the media. A very low percentage of cytotoxicity was measured for treatment of MEM with DMSO, FTI-277, or U0126 (1.42%, 2.62%, and 3.77%), compared with the positive control (bovine heart LDH) provided by the Promega kit.

Activated Erks in hyperplastic tissue. Figure 5 demonstrates the presence of activated Erk1 and Erk2 in the hyperplastic MEM at various time points. There was an increase in activated Erk1 and Erk2 at 1 and 6 h after infection. The level of Erk1 and Erk2 activation then decreased to that of the negative control during the 24–72-h time points. On days 6 and 7, there was a reelevation of Erk1 and Erk2 activation. Total Erk also showed a decrease between 6 and 72 h after bacterial inoculation. The level of total p38 did not change over the time course tested (data not shown).

Expression of Ras isoforms in hyperplastic MEM. PCR products of the appropriate size for all 3 isoforms of Ras were amplified from MEM. H-Ras primers amplified a 392-bp product, K-Ras primers gave a band at 285 bp, and N-Ras primers produced a band at 287 bp (figure 6).

Discussion

The results of the present study support a role for intracellular signaling pathways related to Ras and Erk in MEM hyperplasia. MEMs challenged in vivo with *H. influenzae* demonstrated elevated levels of activated Erk1/Erk2 at specific postinfection time

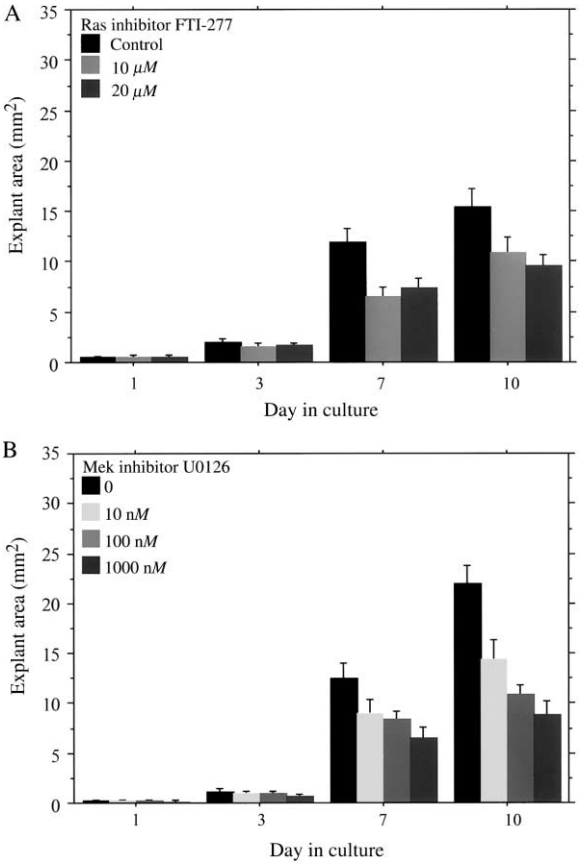

Figure 4. Surface area of nonhyperplastic (no bacterial inoculation) middle-ear mucosa explants cultured with different concentrations of signaling inhibitors. *A,* With farnesyl transferase inhibitor (FTI)–277, significant inhibition was observed at 10 μM ($P < .0002$) and 20 μM ($P < .0001$). *B,* With U0126, significant inhibition was observed at 10 nM ($P < .0001$), 100 nM ($P < .0001$), and 1000 nM ($P < .0001$). Bars, mean; vertical lines, 1 SE.

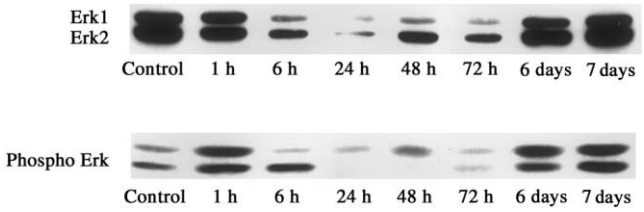

Figure 5. Western blot of total extracellular regulated kinase (Erk) 1 and Erk2 and phosphorylated (Phospho) Erk at various postinoculation times. Total protein was equalized in all lanes. Total Erk showed a decrease between 6 and 72 h after inoculation. Erk activation showed 2 peaks, at 1 h and again at 6–7 days.

points. Likewise, inhibition of Ras signaling, using the farnesyl transferase inhibitor FTI-277, or Erk, using U0126, produced a dose-dependent inhibitory effect on the growth of hyperplastic MEM cells in vitro. FTI-277 also caused a significant inhibitory response on tissue outgrowths of nonhyperplastic MEM in vitro; however, this response was not nearly as extensive as in the hyperplastic tissue. In contrast U0126 showed comparable results on nonhyperplastic and hyperplastic MEMs. The temporal relationship between Erk activation and FTI-277 and U0126 inhibition suggests a complex interaction between Erk and Ras signaling during bacterial OM.

The degree of mucosal growth in vitro was dependent on the postinfection time of the tissue harvested in vivo (figure 1). When harvested at 48 h after infection, the MEM was in the most active state of growth in vitro. For several days, these explants continued to grow at a significantly higher rate than did control tissue and explants harvested at all other postinfection time points. This is consistent with in vivo observations that mucosal hyperplasia is maximal 48–72 h after initiation of experimental OM [4, 8, 36]. The resistance of the tissue to handling also changed over time, with increased fragility peaking at 96 h. This response does not appear to reflect loss of the mucosal epithelium. Magnuson et al. [8] found that the mucosa was thickest at this time point, with several additional layers of epithelial cells. It is possible that this fragility reflects edema and changes in intercellular connections. Both edema and leukocyte extravasation between mucosa cells occur at this time period [8, 11]. With respect to tissue growth, BrdU labeling (figure 2) indicated that the expansion of the explants in culture is a hyperplastic response that consists of both cellular growth and proliferation, as opposed to migration of cells from the original explanted tissue. This hyperplastic response of the MEM appears to be partially dependent on Ras signaling.

Ras is an important link that connects growth factor receptors to the intracellular signal transduction responsible for cell growth and proliferation [37]. Ras activity increases during the proliferation of many cell types [38], whereas inhibition of Ras decreases proliferation and growth [25, 39]. For example, increased Ras processing has been documented in proliferating hepatocytes after partial hepatectomy or after phenobarbital-induced mitogenic liver hyperplasia [40]. Likewise, inhibition of Ras processing has been shown to suppress growth of actively dividing tumor cells from a wide variety of human tissues [41]. Ras farnesylation is required for its transforming activity and takes place on the last 4 aa from the C-terminal end of the protein. The C-terminus consists of a cystine, 2 aliphatic amino acids, and one additional residue. Together, this is known as the CAAX box [25]. The farnesylation inhibitor FTI-277 is a CAAX box peptidomimetic that competes for farnesyl transferase and suppresses the farnesylation and integration of Ras into the cell membrane. Although the non–cell-permeable form of FTI-277, FTI-276, has been shown to inhibit geranyl-geranyl-transferase at high concentrations, FTI-277 is considered a selective inhibitor of farnesyl transferase, because the inhibition of geranylgeranylated Rap1A by FTI-277 does not occur at concentrations $\leq 10\ \mu M$ [30]. The intracellular pathways affected by FTI-277 become less defined at concentrations $>10\ \mu M$. Of course, as is the case with all inhibitors, it is possible that FTI-277 at various concentrations may inhibit other signaling cascades that have not yet been characterized.

The effects of FTI-277 on the growth of cultured hyperplastic and nonhyperplastic MEMs are shown in figures 3 and 4, respectively. Although no significant inhibition of growth occurred at an FTI-277 concentration of 1 μM, both the hyperplastic and nonhyperplastic tissue demonstrated an inhibitory response at 10 and 20 μM FTI-277, with no significant difference in tissue response between these 2 concentrations. This suggests that growth inhibition was saturated at 10 μM. However, as a percentage of the controls, inhibition of hyperplastic mucosal outgrowth was 2–3 times that of the nonhyperplastic tissue (figures 3 and 4), which suggests that Ras activation is more important during mucosal hyperplasia than during unstimulated mucosal proliferation. This point is further emphasized by the observation that FTI-277 at 10 and 20 μM reduced the growth of the bacterially stimulated mucosa to less than that of the nonhyperplastic negative control specimens (figures 3 and 4). This suggests that Ras inhibition essentially eliminated the bacterially-induced mucosal hyperplasia.

The above data have implications for the specific Ras isoform that is predominant in MEM hyperplasia. To date, 3 isoforms (H, K, and N) of Ras have been described in mammalian cells [42]. Our PCR data suggest that all are present in the middle ear. The farnesyl transferase inhibitor FTI-277 has a dose-de-

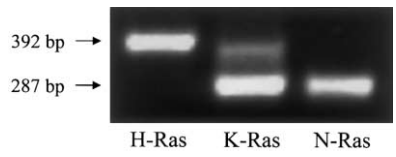

Figure 6. Polymerase chain reaction products of the 3 Ras isoforms, H-Ras, K-Ras, and N-Ras, amplified from middle-ear mucosa 48 h after bacterial inoculation.

pendent specificity for the 3 different Ras isoforms. Lerner et al. [43] found that H-Ras processing is inhibited at concentrations as low as 10 n*M* and is impeded 95% at 3 μM. N-Ras processing can be completely suppressed at FTI-277 concentrations as low as 5 μM. Inhibition of K-Ras processing, however, requires an FTI-277 concentration of at least 10 μM [30, 43]. In the present study, there was no significant difference between the control explants and those treated with FTI-277 at 1 μM (figure 3*A*), a concentration that Lerner et al. [43] found to be more than sufficient to inhibit H-Ras. This suggests that K-Ras and/or N-Ras are the predominant isoforms involved in the hyperplastic response of bacterially stimulated MEM in vitro.

Effector molecules downstream of Ras via the Raf/Mek pathway are the Erks. These MAP kinases have been shown to participate in cellular proliferation during gastrointestinal mucosal regeneration and wound repair [33, 44]. Phosphorylated Erk1 and Erk2 were present in the hyperplastic MEMs examined in the present study (figure 5) and therefore may be responsible for hyperplasia of the MEM. The extent of the Erk phosphorylation should reflect the level of activation, which was dependent on the length of in vivo exposure to *H. influenzae.* The strongest phosphorylation of Erk1 and Erk2 was observed at 1 and 6 h and at 6 and 7 days, suggesting that Erk1 and Erk2 are involved in the MEM response during bacterial OM.

Inhibition by U0126 significantly reduced mucosal hyperplasia, which also supports a role for Erks. However, it should be noted that U0126 had a similar effect on the growth of both normal and bacterially exposed MEMs. Thus, the additional growth caused by bacterial exposure may be less dependent on Erk than on Ras.

Moreover, a comparison of FTI-277 and U0126 inhibition with Erk phosphorylation also suggests that the Ras/Raf/Mek/Erk intracellular pathway may not be responsible for mediating all of the mucosal growth and hyperproliferation suppressed by FTI-277 in culture. The most active growth of the explants was observed at 48 h after infection. This growth was significantly inhibited by FTI-277, suggesting active Ras processing at this time point. In vivo, however, phosphorylated Erk1 and Erk2 were maximally elevated at 1 and 6 h and then again at 6 and 7 days after infection (figure 5). Little activation of Erks was documented at 48 h, where maximal tissue growth was observed in culture (figure 1). This lack of phosphorylated Erk was at least partially due to a change in total Erk at these times. This change was specific to the Erks, because p38 remained constant. Moreover, although U0126 decreased mucosal growth in culture, the effects on bacterially exposed mucosa are not substantially greater than those seen in normal mucosa. The disparity between Ras inhibition and Erk inhibition/activation may be related to the varying functional roles of different Ras isoforms. Previous studies have documented a strong relationship between the processing of H- and N-Ras and the activation of Erks [45–47]. In contrast, K-Ras processing is not as strongly associated with Erk activation [48]. This is consistent with our data, which suggest a role for K-Ras, acting through an Erk-independent pathway, in maintaining the MEM hyperplasia observed in culture. Ras is known to activate downstream pathways other than the Erks, including p120 Ras GAP [49], GEFs for Ral [50], AFG/Canoe [51, 52], RIN1 [53], p38 [54], and phosphatidylinositol 3-kinase (PI3K) [55]. PI3K activation has specifically been linked to the K-Ras isoform [56]. This or other alternate pathways could be involved in MEM hyperplasia. Further investigations will be required to identify the most critical pathways.

Although the present study does not support a dominant role for Erks in the maintenance of bacterially induced mucosal hyperplasia in the 48-h explants, our data by no means exclude them from participation in MEM hyperplasia. Previous studies, in other tissue systems, have demonstrated that the Erk pathway can be critically involved, not only in cellular growth and proliferation, but also in cellular differentiation and senescence. Transient Erk signaling has been shown to be required for proliferation in some cells, but a strong, sustained signal can lead to cell cycle arrest and apoptosis [57–60]. This characteristic of the Erks, in combination with the effects of U0126 and the elevated Erk phosphorylation shown in figure 5, suggest a possible role for the Erk pathway in both the initiation and the resolution of MEM hyperplasia. Magnuson et al. [8] and others [4, 36] have found that MEM proliferation begins ~24 h after the initiation of OM and reaches a maximum at 3–4 days, whereas substantial recovery from hyperplasia occurs by 8 days after inoculation. In the present study, activated Erk1 and Erk2 were significantly elevated at 1–6 h after inoculation, prior to tissue proliferation, followed by a steep decrease. This transient Erk activation might contribute to the initiation of mucosal hyperplasia. Erk phosphorylation was not significantly elevated at 24, 48, and 72 h after innoculation, compared with control MEMs. However, high levels of Erk phosphorylation reoccurred on days 6 and 7, a time point at which OM is beginning to resolve. Sustained reactivation of the Erks at 1 week after infection could contribute to cell cycle arrest and, ultimately, to the resolution of tissue hyperplasia. Erk activation may thus be one of the regulatory pathways involved in returning the MEM to a resting state after the resolution of infection. Of course, the results obtained in in vitro models must be interpreted with caution. The more dynamic situation that occurs in vivo undoubtedly includes events that were not present in our model.

The results of the present study support the involvement of both Ras and the Erks in MEM hyperplasia and may possibly be relevant to treatment of OM. However, the timing of any potential intervention in signaling would be critical. Early application of inhibitors that suppress Ras and/or Erk activation may reduce hyperplasia in the middle ear, decreasing the severity and morbidity of OM. However, introducing inhibitors during the latter stages of infection might interfere with tissue recovery and exacerbate the damage caused by OM. Additionally, even

at saturating levels of FTI-277, some mucosal growth still occurred (figure 3*A*). This suggests the involvement of alternative pathways independent of Ras in MEM hyperplasia and suggests the need for multiple inhibitors to completely block the middle-ear hyperplastic response. A better understanding of which pathways are involved during specific postinfection time points will provide knowledge about the intracellular mechanisms on which to focus potential interventions.

References

1. Junqueira LC, Carneiro J, Kelley RO. Basic histology. Norwalk, CT: Appleton & Lange. **1995**.
2. Koutnouyan HA, Baird A, Ryan AF. Acidic and basic FGF mRNA expression in the middle ear mucosa during experimental acute and chronic otitis media. Laryngoscope **1994**;104:350–8.
3. Ryan AF, A Baird. Growth factors during proliferation of the middle ear mucosa. Acta Otolaryngol **1993**;113:68–74.
4. Lim D, Birck H. Ultrastructural pathology of the middle ear mucosa in serous otitis media. Ann Otol Rhinol Laryngol **1971**;80:838–53.
5. Keithley EM, Krekorian T, Sharp P, Harris JP, Ryan AF. Comparison of immune-mediated models of acute and chronic otitis media. Arch Otorhinolaryngol **1990**;247:247–51.
6. Kuijpers W, van der Beek JMH, Willart ECT. The effect of experimental tubal obstruction on the middle ear. Acta Otolaryngol **1979**;87:345–52.
7. Lowell S, Juhn SK, Giebink GS. Experimental otitis media following middle ear inoculation of nonviable streptococcus pneumoniae. Ann Otol Rhinol Laryngol **1980**;89:479–82.
8. Magnuson K, Hermansson A, Melhus A, Hellstrom S. The tympanic membrane and middle ear mucosa during non-typeable *Haemophilus influenzae* and *Haemophilus influenzae* type b acute otitis media: a study in the rat. Acta Otolaryngol **1997**;117:396–405.
9. Krekorian T, Keithley EM, Takahashi M, Ryan AF, Fierir J, Harris JP. Endotoxin induced otitis media with effusion in the mouse. Acta Otolaryngol **1990**;109:288–99.
10. DeMaria TF, Billy JM, Danahey DG. Growth factors during endotoxin-induced experimental otitis media. Acta Otolaryngol **1996**;116:854–6.
11. Ryan AF, Catanzaro A, Wasserman S, Harris JP. Secondary immune response in the middle ear: physiological, anatomical and immunological observations. Ann Otol Rhinol Laryngol **1986**;95:242–9.
12. Catanzaro A, Ryan AF, Batcher S. The response to human rIL-1, rIL-2 and rTNF in the middle ear of guinea pigs. Laryngoscope **1991**;101:271.
13. Mawson S, Fagan P. Tympanic effusions in children: long-term results of treatment by myringotomy, aspiration, and indwelling tubes. J Laryngol Otol **1972**;86:105–19.
14. Morgan W Jr. Tympanosclerosis. Laryngoscope **1977**;87:1821–5.
15. Kilby D, Richards S, Hart G. Grommets and glue ears: two-year results. J Laryngol Otol **1972**;86:881–8.
16. Sade J. Pathogenesis of attic cholesteatoma: the metaplasia theory. In: McCabe BF, Sade J, Abramson M, eds. Cholesteatoma: first international conference. Birmingham, AL: Aesculapius, **1978**;212–32.
17. Cawthorne T. Chronic adhesive otitis. J Laryngol Otol **1956**;70:559–64.
18. Sheehy J, Brackmann D, Graham M. Cholesteatoma surgery: residual and recurrent disease—a review of 1,024 cases. Ann Otol Rhinol Laryngol **1977**;86:451–62.
19. Palacios SD, Oehl HJ, Rivkin AZ, Aletsee C, Pak K, Ryan AF. Growth factors influence growth and differentiation of the middle ear mucosa. Laryngoscope **2001**;110:874–80.
20. Baird A, Walicke PA. Fibroblast growth factors. Br Med Bull **1989**;45:438–52.
21. Gospodarowicz D. Fibroblast growth factor—chemical structure and biological function. Clin Orthop **1990**;257:231–48.
22. Van Blitterswijk C, Ponec M, Van Muijen G, Wijsman M, Koerten H, Grote J. Culture and characterization of rat middle-ear epithelium. Acta Otolaryngol **1986**;101:453–66.
23. Lemmon MA, Schlessinger J. Regulation of signal transduction and signal diversity by receptor oligomerization. Trends Biochem Sci **1994**;19:459–63.
24. Olson M, Marais R. Ras protein signaling. Semin Immunol **2000**;12:63–73.
25. Berhard E, McKenna W, Hamilton A, et al. Inhibiting ras prenylation increases the radiosensitivity of human tumor cell lines with activating mutations of ras oncogenes. Cancer Res **1998**;58:1754–61.
26. Leonard D. Ras farnesyltransferase: a new therapeutic target. J Med Chem **1997**;40:19.
27. Egan S, Weinberg R. The pathways to signal achievement. Nature **1993**;365, 781–6.
28. Vojtek A, Der CJ. Increasing complexity of the Ras signaling pathway. J Biol Chem **1998**;273:19925–8.
29. Kato K, Der CJ, Buss J. Prenoids and palmitate: lipids that control the biological activity of Ras proteins. Semin Cancer Biol **1992**;3:179–88.
30. Casey P. Protein prenyltransferases. J Biol Chem **1996**;271:5289–92.
31. Lerner E, Qian Y, Blaskovich M, et al. Ras CAAX peptidomimetic FTI-277 selectively blocks oncogenic Ras signaling by inducing cytoplasmic accumulation of inactive Ras-Raf complexes. J Biol Chem **1995**;270:26802–6.
32. Huang C, Chen C, Huang T, Shinoda H. Mediation of signal tranasduction in keratinocytes of human middle ear cholesteatoma by ras protein. Eur Arch Otorhinolaryngol **1996**;253:385–9.
33. Jones M, Tomikawa M, Mohajer B, Tarnawski A. Gastrointestinal mucosal regeneration: role of growth factors. Front Biosci **1999**;4:D303–9.
34. Melhus A, Hermansson A, Akkoyunlu M, Forsgren A, Prellner K. Experimental recurrent otitis media induced by *Haemophilus influenzae:* protection and serum antibodies. Am J Otolaryngol **1995**;16:383–90.
35. Melhus A, Hermansson A, Prellner K. Nontypeable and encapsulated *Haemophilus influenzae* yield different clinical courses of experimental otitis media. Acta Otolaryngol **1994**;114:289–94.
36. Friedmann I. The comparative pathology of otitis media—experimental and human. II. The histopathology of experimental otitis of the guinea pig with particular reference to experimental cholesteatoma. J Laryngol **1955**;69: 588–601.
37. Campbell S, Khosravi-Far R, Rossman K, Clark G, Der C. Increasing complexity of Ras signaling. Oncogene **1998**;17:1395–413.
38. Ewen M. Relationship between ras pathways and cell cycle control. Prog Cell Cycle Res **2000**;4:1–17.
39. Du W, Lebowitz P, Prendergast G. Non-Ras targets of farnesyltransferase inhibitors: focus on Rho. Oncogene **1998**;17:1439–45.
40. Goldsworthy T, Goldsworthy S, Sprankle C, Butterworth B. Expression of myc, fos and Ha-ras associated with chemically induced cell proliferation in the rat liver. Cell Prolif **1994**;27:269–78.
41. Prevost G, Pradines A, Viossat I, et al. Inhibition of human tumor cell growth in vitro and in vivo by a specific inhibitor of human farnesyltransferase: BIM-46068. Int J Cancer **1999**;83:283–7.
42. Barbacid M. ras genes. Annu Rev Biochem **1987**;56:779–827.
43. Lerner E, Zhang T, Knowles D, Qian Y, Hamilton A, Sevti S. Inhibition of the prenylation of K-Ras, but not H- or N-Ras, is highly resistant to CAAX peptidomimetics and requires both a farnesyltransferase and a geranylgeranyltransferase I inhibitor in human tumor cell lines. Oncogene **1997**;15:1283–8.
44. Dieckgraefe B, Weems D, Santoro S, Alpers D. ERK and p38 MAP kinase pathways are mediators of intestinal epithelial wound-induced signal transduction. Biochem Biophys Res Commun **1997**;233:389–94.
45. Senmaru N, Shichinohe T, Takeuchi M, et al. Suppression of Erk activation and in vivo growth in esophageal cancer cells by the dominant negative Ras mutant, N116Y. Int J Cancer **1998**;78:366–71.
46. Qui M, Green S. PC12 cell neuronal differentiation is associated with prolonged p21ras activity and consequent prolonged ERK activity. Neuron **1992**;9:705–17.
47. Plattner R, Gupta S, Khosravi-Far R, et al. Differential contribution of the ERK and JNK mitogen-activated protein kinase cascades to Ras trans-

formation of HT1080 fibrosarcoma and DLD-1 colon carcinoma cells. Oncogene **1999**;18:1807–17.

48. Yip-Schneider M, Lin A, Barnard D, Sweeney C, Marshall M. Lack of elevated MAP kinase (Erk) activity in pancreatic carcinomas despite oncogenic K-ras expression. Int J Oncol **1999**;15:271–9.
49. Yatani A, Okabe K, Polakis P, Halenbeck R, McCormick F, Brown A. ras p21 and GAP inhibit coupling of muscarinic receptors to atrial K^+ channels. Cell **1990**;61:769–76.
50. Feig L, Urano T, Cantor S. Evidence for a Ras/Ral signaling cascade. Trends Biochem Sci **1996**;21:438–41.
51. Van Aelst L, White M, Wigler M. Ras partners. Cold Spring Harb Symp Quant Biol **1994**;59:181–6.
52. Kuriyama M, Harada N, Kuroda S, et al. Identification of AF-6 and canoe as putative targets for Ras. J Biol Chem **1996**;27:607–10.
53. Han L, Colicelli J. A human protein selected for interference with Ras function interacts directly with Ras and competes with Raf1. Mol Cell Biol **1995**;15:1318–23.
54. Matsumoto T, Yokote K, Tamura K, et al. Platelet-derived growth factor activates p38 mitogen-activated protein kinase through a Ras-dependent pathway that is important for actin reorganization and cell migration. J Biol Chem **1999**;274:13954–60.
55. Rodriguez-Viciana P, Warne P, Dhand R, et al. Phosphatidylinositol-3-OH kinase as a direct target of Ras. Nature **1994**;370:527–32.
56. Perugini R, McDade T, Vittimberga F, Callery M. Pancreatic cancer cell proliferation is phosphatidylinositol 3-kinase dependent. J Surg Res **2000**;90:39–40.
57. Serrano M, Lin A, McCurrach M, Beach D, Lowe S. Oncogenic Ras provokes premature cell senescence associated with accumulation of p53 and p161NK4a. Cell **1997**;88:593–602.
58. Sewing B, Wiseman A, Lloyd H, Land. High-intensity Raf signal causes cell cycle arrest mediated by p21Cip1. Mol Cell Biol **1997**;17:5588–97.
59. Olson M, Paterson H, Marshall C. Signals from Ras and Rho GTPases interact to regulate expression of p21 Waf1/Cip1. Nature **1998**;394:295–9.
60. Kauffmann-Zeh A, Rodrigues-Viciana P, Ulrich E, et al. Suppression of c-Myc–induced apoptosis by ras signaling through PI(3)K and PKB. Nature **1997**;385:544.